

Search for muon signal from dark matter annihilations in the Sun with the Baksan Underground Scintillator Telescope for 24.12 years

M.M. Boliev

*Institute for Nuclear Research of Russian Academy of Sciences,
Baksan Neutrino Observatory, Kabardino-Balkariya 400900, Russia
E-mail: boliev2005@yandex.ru*

S.V. Demidov

*Institute for Nuclear Research of Russian Academy of Sciences,
prospect 60-th October 7A, Moscow 117312, Russia.
E-mail: demidov@ms2.inr.ac.ru*

S.P. Mikheyev[†]

*Institute for Nuclear Research of Russian Academy of Sciences,
prospect 60-th October 7A, Moscow 117312, Russia.
E-mail: mikheyev@pcbai10.inr.ruhep.ru*

O.V. Suvorova

*Institute for Nuclear Research of Russian Academy of Sciences,
prospect 60-th October 7A, Moscow 117312, Russia.
E-mail: suvorova@cpc.inr.ac.ru*

ABSTRACT: We present a new dataset analysis of the neutrino experiment at the Baksan Underground Scintillator Telescope with muon energy threshold about 1 GeV for the longest exposure time toward the Sun. In search for a signal from self-annihilations of dark matter particles in the center of the Sun we use an updated sample of upward through-going muons for 24.12 years of live time. No observable excess has been found in measured muons relative to expected background from neutrinos of atmospheric origin. We present an improved data analysis procedure and describe it in detail. We set the 90% C.L. new upper limits on expected neutrino and muon fluxes from dark matter annihilations in the Sun, on the corresponding annihilation rates and cross sections of their elastic scattering off proton.

KEYWORDS: high energy neutrinos, dark matter.

[†]*Dedicated to the memory of Stas Mikheyev.*

Contents

1. Introduction	1
2. Experiment, triggers and sample of upward through-going muons	2
3. The Sun survey during three decades	4
4. Transport of neutrinos produced from dark matter annihilations in the Sun to the Earth	5
5. Results	8
6. Summary	12

1. Introduction

Evidence for a huge amount of missing (that is dark) mass in the Universe comes from observed gravitational effects in astrometry, as it was first discovered by F.Zwicky [1]. The most impressive hints come from measurements of rotation curves of spiral galaxies and gravitational lensing (see Refs. [2, 3, 4, 5] for review) including reconstructed view of the merging process of the bullet cluster [6, 7] which indicates that what is interpreted as dark matter effects can not be explained by some modification of the gravity law. Recent high precision measurements of microwave background anisotropy [8, 9] continue to indicate that the total energy density contains only about 4.6% of baryonic matter while other parts come from non ordinary forms of gravitating matter: dark energy, about 72%, and dark matter (DM), about 23%. The best fit of the results of observational astronomy favours the flat Λ CDM model in cosmology which implies existence of the collisionless nonrelativistic DM in an extension of the Standard Model (SM) of particle physics. These facts generate numerous multi-wavelength searches for relic particles through their possible interactions with ordinary matter by direct and indirect methods. Moreover, several recent results obtained in low background detectors of nuclear recoil reactions [10, 11, 12, 13, 14] and in cosmic ray experiments of γ , e^-e^+ and $p\bar{p}$ measurements (see Ref. [15] for review) indicate on existence of spectral peculiarities which have been interpreted by many authors as an evidence on existence of dark matter. Indirect search for dark matter through neutrino channel is accessible within dataset analysis of neutrino telescopes in their regular observations of local sources like the Sun where DM could be gravitationally trapped and further accumulated for the time of solar system age.

Up-to now there are no hints on excess of neutrino events in the direction towards the Sun as compared with expected background of atmospheric neutrinos at all neutrino telescopes. However, these observations allow to set upper limits on properties of dark matter particles, in particular, upper limits on their annihilation rates in the Sun which under certain assumptions can be translated into upper limits on the cross sections of elastic scattering of dark matter on nucleons. Given the Sun chemical composition with approximately 73% of hydrogen the spin-dependent elastic cross section of dark matter particles on proton appears to be one of the most sensitive quantities in these searches as it can be seen from the latest results from the Super-Kamiokande [16], the IceCube [17] and the ANTARES [18] collaborations.

The Baksan Underground Scintillator Telescope [19] (further referred to as the Baksan or the BUST) has muon energy threshold around 1 GeV allowing for searches for neutrino signal from annihilation of relatively light dark matter in the Sun. Corresponding minimal mass which can be probed at the Baksan is about 10 GeV. Here we present updated results of the Baksan experiment with the statistics twice as compared to the previous ones [20] and with new analysis improved in several ways. First of all, current knowledge of neutrino properties has been fully taken into account. Besides, the previous Baksan results [20, 21, 22] were obtained in the framework of a specific model - MSSM (Minimal Supersymmetric Standard Model) with neutralino as a dark matter candidate (see Ref. [23] for a review). Performing a scan over its parameter space but fixing the mass of dark matter particle conservative upper limits on muon flux and the rate of dark matter annihilation in the Sun have been obtained. In the present work rather than studying a specific theory we follow a present day approach which is applicable to a wider class of models. Namely, one can make an assumption about dominating annihilation channel for dark matter particles in the Sun and then set the limit on the corresponding annihilation rate. This approach allows us to compare the Baksan limits with the results of other neutrino experiments and at the same time it is to a certain extent model independent: having the limits on possible annihilation channels allows one to apply them to a specific model. In our analysis we consider annihilations of dark matter particles into $b\bar{b}$, $\tau^+\tau^-$ and W^+W^- . We use our own C code to simulate neutrino propagation from the point of production in the Sun to the detector level and compare our results with those obtained with the help of WimpSim package [24, 25].

The paper is organized as follows. In Sec. 2 main parameters of the Baksan Underground Neutrino Telescope and levels of neutrino events selection are presented. In Sec. 3 we describe the angular analysis of the upward going muon dataset. In Sec. 4 we describe in details numerical simulations of neutrino propagation and muon signal in the telescope. The results and discussion are presented in Sec. 5. Finally, Sec. 6 contains our conclusions.

2. Experiment, triggers and sample of upward through-going muons

The Baksan Underground Scintillator Telescope is a well known aged neutrino telescope located in one of two underground tunnels of the Baksan Neutrino Observatory. The BUST has 4-pi geometry for detection of penetrating charged particles. The duration of continuous

measurements covers 34 years since December of 1978. Main parameters of the telescope have been presented in details in Refs. [19, 26]. Separation of arrival directions between up and down hemispheres is made by time-of-flight (TOF) method with time resolution 5 ns [27]. It was shown [27] that in 95% of events values of inverse reconstructed particle velocity $1/\beta$ lie in the range of $0.7 \div 1.3$ for single downward going muons. Such interval but with negative sign of velocity is used to select upward going muons generated by neutrino interactions in down hemisphere.

The telescope is located at the altitude 1700 m above sea level in the Baksan valley of the North Caucasus and at the depth 850 hg/cm² under the mountain Andyrchi where the flux of atmospheric downgoing muons is reduced by factor of about 5000, but it is still higher than upgoing muons flux by six orders of magnitude. Trajectories of penetrating particles are reconstructed using the positions of hit tanks, which represent together a system of 3150 liquid scintillation counters of standard type (70 cm \times 70 cm \times 30 cm) in configuration of parallelepiped (17 m \times 17 m \times 11 m). The counters entirely cover all its sides and two horizontal planes inside at the distances 3.6 m and 7.2 m from the bottom. The planes are separated from each other by concrete absorber of radiation length ≈ 160 g/cm². The configuration provides about 1.5° of muon angular resolution for reconstructed trajectories longer than 7 meters.

The angular resolution of the Baksan telescope depends on a ratio of geometrical sizes of whole telescope and individual counter (tank), as well as on selection criteria, in particular, on length of the muon trajectory. The detailed studies have been done previously by Monte Carlo simulations and experimental data sets analysis of single downward going muons, pairs of parallel muons in muon groups [28, 29], the Moon shadowing of the cosmic rays [30, 31], the neutrino local sources studies [32], observations of muons toward the moving sources as for the Cygnus-X3 [28].

The rate of the general trigger of events at the telescope is 17 Hz. There are two special hardware triggers used to select upward going muons [26]. They reduce initial rate of downward going muons approximately by factor of 10^3 . Trigger I covers the zenith angle range $95^\circ \div 180^\circ$ while trigger II selects horizontal muons in the angular range $80^\circ \div 100^\circ$. The hardware trigger efficiency of 99% has been measured with the flux of atmospheric muons [26, 27]. These two triggers select 0.1% of the initial rate, leaving about 1800 events per day for further processing. In the year 2000 the telescope data acquisition system was upgraded and allowed to simplify the trigger system down to one general trigger with the rate of 17 Hz. All raw information is then undergone further selection using off-line reconstruction code.

Selection criteria of neutrino events in the Baksan neutrino experiment has not been changed since the first data analyses [22, 26, 33, 34]. An off-line program reconstructs events and selects those of them which satisfy two simple requirements: presence of only one reconstructed track of penetrating particle and negative value of measured velocity β . In addition, all events with negative values of β have been scanned by the eyes to check possible misinterpretation and there were no observed events within range of $-0.5 \leq \beta \leq 0$. Also it is required that each trajectory has an enter point lower than exit point on a range not less than

the tank size. For trajectories crossing only two scintillator planes (sample of trigger II) we have excluded tracks having azimuthal angles $0^\circ \leq \phi \leq 180^\circ$ from the direction of minimum shallow depth to reduce background from downward going atmospheric muons scattered at large angles in the rock.

The data used for the present analysis have been collected from December of 1978 till November of 2009. In total, during 211275 hours of live time (l.t.) which corresponds to 24.12 years, 1700 events surviving the cuts described above have been collected.

Additional cuts have been applied in order to reject upward-going trajectories that could be mimicked by downward-going atmospheric muon interactions or multiple muons. i) The muon trajectory should have entry and exit points. Thus, stopping muons and neutrino interactions inside the detector are excluded. ii) Muon range inside detector must be larger than 500 g/cm^2 . These criteria cut off particles with energy below $\approx 1 \text{ GeV}$. iii) In the sample of events which passed trigger II, those with entry or exit points closer than 1.5 m to the plane edge are excluded. This cut reduces background from atmospheric muons interactions. iv) Finally, the events with $1/\beta$ in the range of $-1.3 \div -0.7$ only have been accepted.

In total for 24.12 years of live time 1255 events survive all cuts and are used in our further analysis. In Fig. 1 (left) we show the rate of collected measured upward through-going muons for good run periods of each year during all years of observation.

3. The Sun survey during three decades

In search for neutrinos from the dark matter annihilations in the Sun, we analyse distribution of measured events as a function of $\cos \Psi_{\mu-\text{Sun}}$ where $\Psi_{\mu-\text{Sun}}$ is the angle between upward incoming muons and the Sun position. In Fig. 1 (right) the obtained cosine distribution is presented. The mean rate per bin is shown by blue line. We estimate the background expected from atmospheric neutrinos directly from real data using shifted (false) Sun positions. Here we follow our previous analysis [20, 21] where it was shown that this method is compatible with Monte Carlo (MC) simulations of the detector response on modeled atmospheric neutrino interactions in the surrounded rock and muon propagation up to the detector. The acceptance for these muons was calculated with the same requirements for hardware triggers and same set of cuts as for real data. The detector efficiency as a function of muon energy is shown [20] in Fig. 2. Mean energy of simulated atmospheric neutrinos, which produce muons with energy larger 1 GeV for passing through the Baksan telescope, was about 50 GeV [20]. From comparison of data sample for 21.15 years of l.t. [34] and collected MC statistics larger than real data taking by factor of 22 (i.e., in total 460 years) it was found that the ratio of observed total number of events to expected one without neutrino oscillations is $0.87 \pm 0.03(\text{stat.}) \pm 0.05(\text{syst.}) \pm 0.15(\text{theor.})$. The details have been presented in Ref. [34].

At the location of the Baksan telescope ($43,16^\circ\text{N}$ and $42,41^\circ\text{E}$) the Sun is seen in average about half of time per day during a year in both hemispheres; in Fig. 3 (left) we show the integral rate of 1255 selected upward through going muons as a function of zenith angle of the Sun for the BUST measured time of good data periods (red points with error bars)

and expected one for the detector runtime (blue histogram). The later is normalized to this number of events. In calculation of the positions of the Sun we apply the Positional Astronomy Library [35]. Performing the chi-square goodness-of-fit test we obtain a value of $\chi^2/d.o.f. = 10.38/19$. It means our multi-years measurements reproduce the Sun full-year passing track with a good accuracy. That is the base for our further analysis.

Potentially, the neutrinos from dark matter annihilations in the Sun can be found at night time when the Sun is below horizon. We compare zenith distributions of neutrino events coming at nightly (N) and daily (D) time. Corresponding day-to-night asymmetry, $\frac{N-D}{N+D}$ is shown in Fig. 3 (left) and no significant difference between these data samples has been observed. Angular distribution for “night” neutrinos is presented in Fig. 4 (left). Note, that our sample contains only upgoing events and the number of events in the bin corresponding to the direction of the Sun $\cos \Psi_{\mu-Sun} = 1$ remains the same as in Figure 1 (right). For “night” neutrinos, we compare cosine distribution in Fig. 4 (left) and integrated angular distribution in Fig. 4 (right) with measured background which has been obtained from averaged distribution of six cases of false Sun positions shifted along the ecliptic. In Fig. 4 (right), the value of cone half-angle γ toward the Sun is shown on abscissa. We observe no excess of events coming from the Sun. Assuming Poisson statistics for both expected background N_B and observed events N_{obs} we obtain 90% C.L. upper limits on additional number of signal events N_S^{90} as follows [36]:

$$C.L. = 1 - \frac{e^{-(N_B+N_S^{90})} \sum_0^{N_{obs}} \frac{(N_B+N_S^{90})^n}{n!}}{e^{-N_B} \sum_0^{N_{obs}} \frac{N_B^n}{n!}}. \quad (3.1)$$

Corresponding upper limits N_S^{90} for each integer value of cone half-angles in interval $1 \div 25^\circ$ are also shown in Fig. 4 (right). The choice of the cone half-angle depends on the mass of dark matter particle and on particular annihilation channel. We discuss it in Section 5.

4. Transport of neutrinos produced from dark matter annihilations in the Sun to the Earth

In this Section we describe numerical procedure which we use to simulate muon signal in the BUST resulting from dark matter annihilations in the Sun. For this purpose the well known WimpSim package is available [24, 25]. However, to have more flexibility we use our own C code for MC simulation of neutrino propagation from the center of the Sun to the level of the Baksan detector. Our general scheme of MC simulations is very similar to that of WimpSim which is very well described in Ref. [25]. They only differ in several details to be discussed in a moment.

In general, the initial spectrum of (anti)neutrino from dark matter annihilations in the Sun is a mixture of inclusive (anti)neutrino spectra from different annihilation channels $\frac{dN_{\nu_i}}{dE_\nu} = \sum_i B_i \frac{dN_{\nu_j}^i}{dE_\nu}$, where $\frac{dN_{\nu_j}^i}{dE_\nu}$ is the energy spectrum of j -th type of (anti)neutrino produced in i -th type of annihilation channel. The quantities B_i are the branching ratios of different channels

which can be calculated given a model for dark matter candidate. Below we simulate neutrino propagation for several values of masses of dark matter particle from 10 GeV to 1 TeV for three dominant annihilation channels: $b\bar{b}$, $\tau^-\tau^+$ or W^+W^- . The channel $b\bar{b}$ represents an example of “soft” spectrum while W^+W^- and $\tau^+\tau^-$ are examples of “hard” spectra.

We do not calculate the neutrino spectra at the production point in the Sun for each annihilation channel by ourselves but take them from Ref. [37]. We check that they coincide with a good accuracy with those obtained with the help of WimpSim package except for small deviations in spectra for ν_τ and $\bar{\nu}_\tau$. During the propagation of neutrinos from the center of the Sun to the level of the detector we take into account three-flavor neutrino oscillations in the vacuum, the Sun and Earth including matter effects, absorption of neutrinos due to charged current (CC) interactions with the interior of the Sun and Earth and the change of the energy spectrum due to neutrino neutral current (NC) elastic scattering and τ -regeneration.

Neutrino oscillations in 3×3 scheme are implemented according to the algorithm described in Refs. [38, 39]. According to this scheme evolution operator analytically calculated for the case of constant medium density is applied to the neutrino wave function. For the case of varying density of the Sun one can subdivide the neutrino path into sufficiently small intervals. Considering the medium density inside each interval as a constant the total evolution operator can be approximated as product of the evolution operators corresponding to the sequence of intervals. We use solar model of Ref. [40]. For parameters of neutrino mixing matrix we use the following values

$$\begin{aligned}\Delta m_{21}^2 &= 7.62 \cdot 10^{-5} \text{ eV}^2, \quad |\Delta m_{31}^2| = 2.55 \cdot 10^{-3} \text{ eV}^2, \\ \delta_{CP} &= 0, \quad \sin^2 \theta_{12} = 0.32, \quad \sin^2 \theta_{23} = 0.49, \quad \sin^2 \theta_{13} = 0.026,\end{aligned}\tag{4.1}$$

which lie within 2σ range of experimentally allowed values assuming normal hierarchy for neutrino masses [41].

Our code follows straight trajectories of individual neutrinos produced at some point near the center of the Sun which is simulated according to the distribution [37, 42]

$$n(r) = n_0 \exp(-r^2/R_{\text{DM}}^2), \text{ where } R_{\text{DM}} = 0.01 R_\odot \sqrt{100 \text{ GeV}/m_{\text{DM}}}.\tag{4.2}$$

To propagate neutrinos from the production point we calculate the interaction length as

$$L_{\text{int}}(E_\nu) = \frac{1}{n_n (\sigma_n^{CC}(E_\nu) + \sigma_n^{NC}(E_\nu)) + n_p (\sigma_p^{CC}(E_\nu) + \sigma_p^{NC}(E_\nu))},\tag{4.3}$$

which depends on neutron and proton number densities in the Sun n_n and n_p , respectively, and the corresponding CC and NC neutrino cross sections on nucleons $\sigma_{n,p}^{CC}$ and $\sigma_{n,p}^{NC}$. Neutrino-nucleon DIS total cross sections and corresponding energy and angular distributions are calculated according to the expressions presented in Ref. [43] using CTEQ6 [44] parton distribution functions. Inside the Sun, we choose the step size δr as the smallest between R_\odot/F and L_{int}/F where $F = 300$ for $E_\nu \geq 100 \text{ GeV}$ and $F = 3000$ for $E_\nu < 100 \text{ GeV}$. Smaller steps at lower energies are required to take into consideration smaller oscillation length. We

check that total accuracy in neutrino fluxes obtained using these step sizes is better than 1%. Then, we calculate the probability for neutrino to have an interaction during this small step δr : $P = 1 - \exp(-\delta r/L_{int})$. After that we simulate the interaction process and if it takes place we determine its type (CC or NC, proton or neutron) with the probabilities according to corresponding cross sections and proton/neutron densities. When calculating CC neutrino-nucleon cross sections we include nonzero value of τ -lepton mass while electron and muon are considered as massless. In NC scattering process the flavor structure of neutrino wave function is left unchanged. Neutrino energy after this interaction is simulated according to the corresponding differential cross section. For CC interactions the flavor of neutrino also has to be simulated and in the case of ν_e and ν_μ neutrinos we just drop them from the flow. For ν_τ we simulate the energy of resulting τ -lepton. Then the secondary neutrinos resulting from τ -decay are considered following procedure described in Appendix of Ref. [45] which is somewhat different from WimpSim implementation of this process¹.

We check results obtained by our code for neutrino differential fluxes at the level of the Earth (1 a.u.) with that of obtained by WimpSim for the same spectra of neutrino at production in the Sun calculated using WimpSim. The comparison is presented in Figs. 5, 6 and 7 for three different annihilation channels and different masses of dark matter particle. The results agree with each other sufficiently well.

High energy muons to be detected in neutrino telescope are produced in CC interactions of neutrinos in the rock just below the detector. The muons lose their energies during their passage from the production point to the detector. The average muon energy loss is usually parametrized by the following formula

$$\left\langle \frac{dE}{dz} \right\rangle = -(\alpha(E) + \beta(E)E)\rho, \quad (4.4)$$

where ρ is the density of the rock and the quantity $\alpha(E)$ corresponds to ionization energy loss while $\beta(E)$ accounts for bremsstrahlung, photonuclear interactions and pair production. We note that stochastic energy losses could be important for masses of dark matter particles $m_{DM} \gtrsim 1$ TeV (see, e.g. [46, 47]), however, we do not consider them in our calculations. We take into account the energy dependence of $\alpha(E)$ and $\beta(E)$ to simulate the muon propagation in the rock. In the interval $1 \div 1000$ GeV of muon energies these coefficients change [48] from $1.8 \cdot 10^{-3}$ to $2.7 \cdot 10^{-3}$ GeV \cdot cm²/g for $\alpha(E)$ and from $0.8 \cdot 10^{-6}$ to $3.9 \cdot 10^{-6}$ cm²/g for $\beta(E)$. Having rather moderate energy dependence in $\alpha(E)$ and $\beta(E)$ in many calculations constant values for these quantities are used, for instance the values $\alpha(E) \approx 2.2 \cdot 10^{-3}$ GeV \cdot cm²/g and $\beta(E) \approx 4.4 \cdot 10^{-6}$ cm²/g for the rock are used in WimpSim. One could expect, that for low energies $E_\mu \lesssim 20$ GeV neglecting energy dependence for these coefficients leads to shorter muon ranges and some underestimate of muon flux. At the same time at high energies as $E_\mu \gtrsim 200 \div 300$ GeV it should result in longer muon ranges and weak overestimate of muon flux. In Fig. 8 we compare the both resulting muon energy spectra $d\Phi_\mu/dE_\mu$ calculated

¹Secondary neutrinos contribute only a small part of total neutrino flux and the differences between the two approaches are not meaningful. We thank Joakim Edsjö for correspondence on this point.

without and with energy dependence in $\alpha(E)$ and $\beta(E)$ using values tabulated in Ref. [48]. We see that the obtained results confirm expectations discussed above. Generally, we find that the correction due to the energy dependence of $\alpha(E)$ and $\beta(E)$ can reach 18% to the resulting muon flux in the rock from $b\bar{b}$ annihilation channel for $m_{\text{DM}} = 10$ GeV and about 2-3% to one from annihilation into W^+W^- for $m_{\text{DM}} = 1000$ GeV. So, the effect is more pronounced at low energies. In Fig. 9 (left) we show the ratio of muon ranges $R_\mu(E, E_{th})/R_\mu^{\text{approx}}(E, E_{th})$ where $R_\mu(E, E_{th})$ is calculated from Eq. (4.4) taking into account energy dependence in $\alpha(E)$ and $\beta(E)$ while $R_\mu^{\text{approx}}(E, E_{th})$ is obtained for constant values $\alpha(E) \approx 2.2 \cdot 10^{-3}$ GeV·cm²/g and $\beta(E) \approx 4.4 \cdot 10^{-6}$ cm²/g. As a cross-check we also verify our simulations of muon flux by comparison with an analytical expressions available for constant values of $\alpha(E)$ and $\beta(E)$ (see e.g. Ref. [49]). In simulation of the muon flux from dark matter annihilation in the Sun we use the energy dependent coefficients $\alpha(E)$ and $\beta(E)$, taking into account slight widening of muon angle distribution due to multiple Coulomb scattering [23].

5. Results

The upper limits on the number of signal events N_S^{90} obtained from the results of the Baksan Underground Scintillator Telescope (see Section 3) can be used to put the 90% upper limit on the flux Φ_μ of muons with energies higher then 1 GeV from the dark matter annihilation rate. This recalculation can be schematically written as

$$\Phi_\mu(90\% \text{ C.L.}) = \frac{N_S^{90}}{\epsilon \times S_{\text{eff}} \times T} \quad , \quad (5.1)$$

where T is the live time, ϵ is a fraction of signal events inside corresponding cone half-angle and S_{eff} is effective area of Baksan telescope in the direction of the expected signal which is averaged with Sun directions and also includes the muon detection efficiency [20, 50]. Corresponding effective exposure towards the Sun amounts to 0.49×10^{15} cm² · s.

The next step of the calculation is choice of a value of the cone half-angle. Here we can explore obvious difference in angular distribution of signal and background events. While muons from atmospheric neutrinos are distributed nearly isotropic over the sky, the angular distribution of muons from dark matter annihilation is expected to be correlated with the direction of the Sun. The angular spread of the signal muons is determined by the hardness of neutrino spectra coming down to the Earth which in turn depends on the DM mass and annihilation channel. Angular properties of the telescope result in additional widening which we take into account with Gaussian distribution over the direction of incoming muon with incorporated angular resolution. The strategy used in the previous analysis [20] consisted of choosing the cone half-angle which contains 90% of events of upgoing muons expected from dark matter annihilations in the Sun. However, one can try to optimize the value of cone half-angle to reach the most stringent expected upper limits. For this purpose we make use of model rejection factor (or MRF) approach [51]. We construct the quantity given by the r.h.s of Eq. (5.1) in which the upper limits on the number of signal events N_S^{90} are replaced by

the upper limits averaged over number of observed events using Poisson distribution, \bar{N}_S^{90} . In this quantity \bar{N}_S^{90} , ϵ and S_{eff} depend on the value of cone half-angle γ . Then, we minimize it with respect to γ and find the optimal value for this angle. The obtained half-cone angles for three annihilation channels $b\bar{b}$, $\tau^+\tau^-$ and W^+W^- in dependence on DM mass are shown in Fig. 9 (right). Found values of cone half-angles are used to calculate the upper limits at 90% C.L. on the number of signal events N_S^{90} and muon flux from the Sun Φ_μ using Eqs. (3.1) and (5.1).

The muon flux is related to the dark matter annihilation rate Γ_A in the Sun as follows

$$\Phi_\mu = \frac{\Gamma_A}{4\pi R^2} \times \sum_{\nu_j} \int_{E_{th}}^{m_{DM}} dE_{\nu_j} P(E_{\nu_j}, E_{th}) \frac{dN_{\nu_j}}{dE_{\nu_j}}, \quad (5.2)$$

where $R = 1$ a.u., dN_{ν_j}/dE_{ν_j} is the spectrum of j -th type neutrino at the Sun surface, $P(E_{\nu_j}, E_{th})$ is the probability to detect muon with energy $E_\mu > E_{th} = 1$ GeV from ν_j neutrino with energy E_{ν_j} after its oscillations and propagation from the Sun surface while the sum goes over all types of neutrino and antineutrino. The probability $P(E_{\nu_j}, E_{th})$ has been calculated numerically as described in the Section 4 for several masses of dark matter particles and annihilation channels $b\bar{b}$, $\tau^+\tau^-$ and W^+W^- .

In the case when the processes of dark matter capture and annihilations in the Sun reach exact equilibrium during time intervals much less than age of the solar system, 4.5 Giga years, the annihilation rate Γ_A should be equal to a half of capture rate determined by scattering cross sections of dark matter particles off solar matter. In that case, annihilation rate can be divided into two parts corresponding to either spin-dependent (SD) or spin-independent (SI) type of contribution to neutralino-nuclei interactions as follows

$$\Gamma_A = \Gamma_A(\sigma_{SI}) + \Gamma_A(\sigma_{SD}), \quad (5.3)$$

where $\Gamma_A(\sigma_{SI})$ and $\Gamma_A(\sigma_{SD})$ are the parts of equilibrium annihilation rate determined by either SI or SD interactions. Using the upper limits on the dark matter annihilation rate in the Sun and hypothesis about exact equilibrium between capture and annihilation processes we can set conservative upper limits on SD and SI elastic cross section of dark matter particles on proton [52]. To reach this goal we use recalculation procedure described in [53] where we obtained corresponding coefficients in the following expressions

$$\sigma_{SD}^{UppLim}(m_\chi) = \lambda^{SD}(m_\chi) \cdot \Gamma_A^{UppLim}(m_\chi) \quad (5.4)$$

$$\sigma_{SI}^{UppLim}(m_\chi) = \lambda^{SI}(m_\chi) \cdot \Gamma_A^{UppLim}(m_\chi) \quad (5.5)$$

as functions of neutralino mass m_χ . In obtaining $\lambda^{SD}(m_\chi)$ and $\lambda^{SI}(m_\chi)$ we assumed 0.3 GeV/cm³ for the local density of dark matter and 270 km/s for root-mean-square of the velocity dispersion. For other details we refer reader to Ref. [53]. We note that in [53] we used simplified solar model which allows to calculate the capture rate analytically [54]. To be consistent with the present study we recalculate the coefficients λ^{SD} and λ^{SI} for solar

model [40] which results in changes of these coefficients within 10% for SD cross section and within 15% for SI.

A possible influence of systematic effects on the number of observed upward going muons have been tested during all years of the telescope measurements. At the Baksan telescope there is implemented a system of continuous online and offline diagnostics of each detector elements and electronic channels, as well a regular recovering work at the telescope planes one day in a week. The measurements have shown [22] that the spread in threshold settings and the PMTs gain is $\approx 10\%$ and the fraction of dead tanks is about 0.5% over the period of the observation. In a mean time the energy thresholds of each of 3150 detectors have been tuned in an equal small magnitude 8 MeV, while energy release of a relativistic particle is at least six times larger. Thus possible macrofluctuations in any tank were not seen by experimental monitoring of a single muon rate from upper hemisphere [30, 31], while a tiny effect were observed due to enough level of stability in the settings of the Baksan multiyears measurements. It was shown [55] the season variations in observed rate of downgoing muons with magnitude value about 1% over all visible part of the sky. As known, these variations arise from changes of stratosphere temperature. Instability of the detector parameters during a long term operation of the telescope has been studied using Monte Carlo simulations on the variation of PMTs gain ($\approx 10\%$), the spread in setting of thresholds ($\approx 10\%$), and time off-set of PMTs (≈ 2 ns) as well as dead tanks ($\approx 1\%$) [20, 22]. It was found that the number of detected events changes by about 1% given a variation of 10% in the PMTs gain and discrimination thresholds. In the measurements of upward going muons by TOF method the time resolution of the telescope plays a more important role. The time resolution is determined by intrinsic properties of the scintillator counters and PMTs and by the accuracy in adjusting the time off-set of each tank. Before the telescope operation all counters have been adjusted to an identical value of delay so that the maximal spread of time off-sets appeared to be less than 2 ns. Continuous monitoring of the time off-sets of all tanks and their online performance shows that the spread increases and a tail at the level of $\approx 2\%$ appears with time [20, 22]. This type of instability is considered as the main source of systematic uncertainties and is under continuous studying. The systematic uncertainties of 8% have been evaluated by means of detector acceptance simulations, varying parameters relevant to the observation of flux of upward going muons.

Another sources of systematic uncertainties are related to estimation of the background and simulation of the signal. Determination of the background using shifted Sun positions results in uncertainty about 3%. The extensive study of systematic uncertainties associated to neutrino properties have been done. We perform MC simulation of resulting muon flux using different oscillation parameters (within 1σ range). In this study systematic uncertainties in the muon flux are found to be of 8% for $\tau^+\tau^-$ channel and of 5% for both W^+W^- and $b\bar{b}$ channels regardless of neutrino energy. Larger uncertainty for $\tau^+\tau^-$ indicates considerable impact of neutrino oscillations in the case of this annihilation channel (see also discussion of Fig. 10 (right) further in the Section). Further, we vary neutrino-nucleon cross sections using for their uncertainties the results presented in Ref. [56] extrapolated for the case of low

energy neutrinos ($E_\nu < 50$ GeV). Simulating resulting muon flux we have found a spread of 10% (4%) for dark matter mass 10 (1000) GeV. There is a considerable contribution from quasi-elastic neutrino interactions to neutrino-nucleon cross section in the low energy range $\lesssim 5$ GeV of neutrino which could be up to 50% as it was shown, for example, in [43] and which is important for signal simulation in the case of the small DM masses about 10 GeV. We do not consider these contributions here; their inclusion should increase total neutrino-nucleon cross section and results in amplification of the signal and therefore in more stringent upper limits. Thus, our limits for low masses are only conservative. Other uncertainties entering the recalculation to the upper limits on SD and SI cross sections are related to nuclear form-factors, solar composition, influence of planets on capture of dark matter particles, structure of the dark matter halo and the dark matter velocity distribution and they are discussed in Refs. [52, 57]. Also we note that recent studies indicate a somewhat higher value of the local dark matter density, closer to 0.4 GeV/cm^3 [58]. However, this increase will make our limits only stronger.

Incorporation of systematic uncertainties into the final results on the mentioned upper limits has been performed by the method of Cousins & Highland [59]. The results for upper limits on quantities discussed above are collected in Table 1 for several masses of dark matter and for chosen annihilation channels. Here we present obtained optimized values of the half-cone angle γ and the upper limits at 90% C.L. on following quantities: the number of signal events N_S^{90} , muon flux from the Sun Φ_μ in the rock, annihilation rate in the Sun Γ_A , the spin-dependent $\sigma_{\chi p}^{SD}$ and spin-independent $\sigma_{\chi p}^{SI}$ scattering cross sections of dark matter particle off proton and also upper limits on neutrino fluxes Φ_ν integrated from energy $E_\nu = 1$ GeV.

In Fig. 10 (left) are shown the 90% C.L. upper limits on muon fluxes from the Baksan's data for the annihilation channels W^+W^- , $b\bar{b}$ and $\tau^+\tau^-$ along with corresponding limits of Super-Kamiokande [16], IceCube [17] and ANTARES [18]. Typically, for indirect searches with neutrino telescopes the annihilation channel $\tau^+\tau^-$ are not considered separately from W^+W^- to set limits on dark matter properties. However, the difference between neutrino spectra from DM annihilation into $\tau^+\tau^-$ and W^+W^- plays an important role. In spite of the fact that the limits on muon fluxes are approximately the same for W^+W^- and $\tau^+\tau^-$, the limits on SD cross section (and on the corresponding annihilation rate) are quite different for these two channels as one can see in Figs. 11. The explanation of this fact resides partly in the effect of neutrino oscillations: the enhancement due to this effect for $\tau^+\tau^-$ channel is considerably larger than for the case of W^+W^- channel. This is illustrated in Fig. 10 (right) where the ratio of muon fluxes with and without oscillation is shown for three annihilation channels depending on mass of dark matter. Another important effect is a breaking "democracy" in average number of high energy neutrinos per one act of dark matter annihilations: for $\tau^+\tau^-$ pairs it is larger in a factor of $2 \div 3$ than for W^+W^+ or $b\bar{b}$ channels. It can be seen in Fig. 10(right) that neutrino oscillations result in a decrease of muon flux from $b\bar{b}$ annihilation channel, which is expected to be dominating at lighter neutralino masses. At the same time the muon flux from W^+W^- annihilations is enhanced. And finally, using $\tau^+\tau^-$ channel allows to extend the upper limits on SD cross section for "hard" type of neutrino spectra to

lower masses of dark matter.

The Baksan 90% C.L. upper limits on SD cross section are shown in Fig. 11 in comparison with experimental results from direct and indirect DM searches. Here we show recent limits of Super-Kamiokande [16], IceCube [17], ANTARES [18, 61, 62], PICASSO [63], KIMS [64], SIMPLE [65], CMS [66] and ATLAS [67] collaborations. A signal range of DAMA [10, 11] experiment is also depicted. Similarly, the Baksan 90% C.L. upper limits on SI cross section are presented in Fig. 12 in comparison with results of IceCube [17], ANTARES [18], DAMA [10, 11], CoGeNT [13], XENON100 [68] and CDMS [12]. Note that the hard channel for the IceCube limits shown in these figures is assumed annihilation into W^+W^- for $m_{DM} > m_W$ and into $\tau^+\tau^-$ otherwise. As one can see from the Figures the Baksan has the strongest limits at low DM masses for $\tau^+\tau^-$ annihilation channel as compared to the other neutrino telescopes.

Let us note, that the indirect limits on SD and SI cross sections are not fully model independent. The limits of neutrino telescopes strongly rely on hypothesis about equilibrium between capture and annihilation processes with dark matter particles in the Sun. However, the equilibrium condition is fulfilled in most of the dark matter scenarios. As for the impressive collider bounds by CMS [66] and ATLAS [67] collaborations on dark matter interactions they are obtained by a recalculation from direct limits on cross sections of dark matter pair production in association with di-jet and missing transverse energy. There are also similar collider bounds from searches using photon and missing transverse energy signature [69, 70]. This recalculation [71, 72, 73] is based on the fact that the diagrams describing the process of dark matter pair production in pp -collisions and elastic scattering process of DM off proton are related by crossing symmetry. However, these procedure and corresponding indirect bounds on SI and SD cross sections are very model dependent because of different kinematics of these processes. The collider bounds especially weaken in the models when dark matter interacts with quarks via light mediators [71, 72, 73] which is explained by completely different scaling of dark matter pair production and dark matter -nucleon scattering cross sections with c.o.m. energy and mass of mediator. Therefore, collider limits on SI and SD elastic cross sections of dark matter particle off proton should be interpreted with care. Finally, we stress that given a particular model different kinds of experiments on DM searches give complementary bounds on the properties of dark matter particles.

6. Summary

We have performed updated analysis of indirect dark matter search with the Baksan Underground Scintillator Telescope data for 24.12 years of live time. In search for an excess of upward going muons in the direction toward the Sun we do not observe any significant deviation from expected atmospheric background. We have presented the 90% C.L. upper limits on spin-dependent and spin-independent elastic cross section of dark matter on proton assuming particular annihilation channels $b\bar{b}$, W^+W^- and $\tau^+\tau^-$. These limits have been derived from the limits on muon fluxes and annihilation rates for dark matter masses in the

$m_{\text{DM}}, \text{GeV}$	channel	γ, deg	N_s^{90}	$\Phi_\mu, \text{cm}^{-2} \text{s}^{-1}$	Γ_A, s^{-1}	$\sigma_{\chi p}^{SI}, \text{pb}$	$\sigma_{\chi p}^{SD}, \text{pb}$	$\Phi_{\nu\mu}, \text{cm}^{-2} \text{s}^{-1}$
10.0	$b\bar{b}$	15.0	9.6	$4.9 \cdot 10^{-14}$	$3.3 \cdot 10^{26}$	$1.2 \cdot 10^{-3}$	$7.0 \cdot 10^{-2}$	0.021
	$\tau^+ \tau^-$	11.7	6.9	$2.7 \cdot 10^{-14}$	$8.1 \cdot 10^{24}$	$2.9 \cdot 10^{-5}$	$1.7 \cdot 10^{-3}$	0.0022
30.0	$b\bar{b}$	10.7	4.6	$1.7 \cdot 10^{-14}$	$1.0 \cdot 10^{25}$	$6.2 \cdot 10^{-5}$	$1.0 \cdot 10^{-2}$	$9.4 \cdot 10^{-4}$
	$\tau^+ \tau^-$	7.4	4.1	$1.3 \cdot 10^{-14}$	$4.1 \cdot 10^{23}$	$2.4 \cdot 10^{-6}$	$4.0 \cdot 10^{-4}$	$1.2 \cdot 10^{-4}$
50.0	$b\bar{b}$	8.8	4.2	$1.4 \cdot 10^{-14}$	$3.6 \cdot 10^{24}$	$3.2 \cdot 10^{-5}$	$8.2 \cdot 10^{-3}$	$3.4 \cdot 10^{-4}$
	$\tau^+ \tau^-$	6.4	4.4	$1.4 \cdot 10^{-14}$	$1.6 \cdot 10^{23}$	$1.4 \cdot 10^{-6}$	$3.6 \cdot 10^{-4}$	$4.7 \cdot 10^{-5}$
70.0	$b\bar{b}$	7.8	4.6	$1.5 \cdot 10^{-14}$	$2.0 \cdot 10^{24}$	$2.6 \cdot 10^{-5}$	$8.5 \cdot 10^{-3}$	$2.1 \cdot 10^{-4}$
	$\tau^+ \tau^-$	5.8	4.7	$1.4 \cdot 10^{-14}$	$8.6 \cdot 10^{22}$	$1.1 \cdot 10^{-6}$	$3.6 \cdot 10^{-4}$	$2.6 \cdot 10^{-5}$
90.0	$b\bar{b}$	7.3	4.0	$1.3 \cdot 10^{-14}$	$1.2 \cdot 10^{24}$	$2.0 \cdot 10^{-5}$	$7.9 \cdot 10^{-3}$	$1.2 \cdot 10^{-4}$
	$\tau^+ \tau^-$	5.4	3.9	$1.1 \cdot 10^{-14}$	$4.5 \cdot 10^{22}$	$7.6 \cdot 10^{-7}$	$3.0 \cdot 10^{-4}$	$1.3 \cdot 10^{-5}$
	$W^+ W^-$	5.5	3.8	$1.1 \cdot 10^{-14}$	$1.0 \cdot 10^{23}$	$1.7 \cdot 10^{-6}$	$6.9 \cdot 10^{-4}$	$1.2 \cdot 10^{-5}$
100.0	$b\bar{b}$	7.1	4.1	$1.3 \cdot 10^{-14}$	$1.0 \cdot 10^{24}$	$1.9 \cdot 10^{-5}$	$8.4 \cdot 10^{-3}$	$1.0 \cdot 10^{-4}$
	$\tau^+ \tau^-$	5.3	3.9	$1.1 \cdot 10^{-14}$	$3.8 \cdot 10^{22}$	$7.1 \cdot 10^{-7}$	$3.1 \cdot 10^{-4}$	$1.1 \cdot 10^{-5}$
	$W^+ W^-$	5.4	3.8	$1.1 \cdot 10^{-14}$	$8.7 \cdot 10^{22}$	$1.6 \cdot 10^{-6}$	$7.1 \cdot 10^{-4}$	$9.4 \cdot 10^{-6}$
200.0	$b\bar{b}$	5.9	4.6	$1.4 \cdot 10^{-14}$	$3.9 \cdot 10^{23}$	$1.7 \cdot 10^{-5}$	$1.2 \cdot 10^{-2}$	$3.9 \cdot 10^{-5}$
	$\tau^+ \tau^-$	4.4	3.2	$8.7 \cdot 10^{-15}$	$9.9 \cdot 10^{21}$	$4.4 \cdot 10^{-7}$	$3.0 \cdot 10^{-4}$	$2.7 \cdot 10^{-6}$
	$W^+ W^-$	4.3	3.2	$8.5 \cdot 10^{-15}$	$2.4 \cdot 10^{22}$	$1.1 \cdot 10^{-6}$	$7.2 \cdot 10^{-4}$	$2.4 \cdot 10^{-6}$
300.0	$b\bar{b}$	5.4	3.9	$1.1 \cdot 10^{-14}$	$1.8 \cdot 10^{23}$	$1.5 \cdot 10^{-5}$	$1.2 \cdot 10^{-2}$	$2.0 \cdot 10^{-5}$
	$\tau^+ \tau^-$	4.1	3.6	$8.3 \cdot 10^{-15}$	$5.4 \cdot 10^{21}$	$4.7 \cdot 10^{-7}$	$3.2 \cdot 10^{-4}$	$1.5 \cdot 10^{-6}$
	$W^+ W^-$	4.0	3.3	$8.4 \cdot 10^{-15}$	$1.4 \cdot 10^{22}$	$1.1 \cdot 10^{-6}$	$9.5 \cdot 10^{-4}$	$1.4 \cdot 10^{-6}$
500.0	$b\bar{b}$	4.9	4.0	$1.1 \cdot 10^{-14}$	$9.8 \cdot 10^{22}$	$1.7 \cdot 10^{-5}$	$1.8 \cdot 10^{-2}$	$1.0 \cdot 10^{-5}$
	$\tau^+ \tau^-$	3.9	3.3	$8.6 \cdot 10^{-15}$	$5.6 \cdot 10^{21}$	$5.6 \cdot 10^{-7}$	$5.9 \cdot 10^{-4}$	$8.4 \cdot 10^{-7}$
	$W^+ W^-$	3.5	3.3	$8.3 \cdot 10^{-15}$	$9.3 \cdot 10^{21}$	$1.6 \cdot 10^{-6}$	$1.7 \cdot 10^{-3}$	$8.4 \cdot 10^{-7}$
700.0	$b\bar{b}$	4.6	3.1	$8.8 \cdot 10^{-15}$	$5.9 \cdot 10^{22}$	$1.7 \cdot 10^{-5}$	$1.8 \cdot 10^{-2}$	$5.9 \cdot 10^{-6}$
	$\tau^+ \tau^-$	3.8	3.3	$8.3 \cdot 10^{-15}$	$2.5 \cdot 10^{21}$	$7.6 \cdot 10^{-7}$	$8.8 \cdot 10^{-4}$	$6.4 \cdot 10^{-7}$
	$W^+ W^-$	3.7	3.3	$8.7 \cdot 10^{-15}$	$7.9 \cdot 10^{21}$	$2.5 \cdot 10^{-6}$	$2.9 \cdot 10^{-3}$	$6.7 \cdot 10^{-7}$
900.0	$b\bar{b}$	4.5	3.1	$8.8 \cdot 10^{-15}$	$6.2 \cdot 10^{22}$	$3.0 \cdot 10^{-5}$	$3.7 \cdot 10^{-2}$	$6.1 \cdot 10^{-6}$
	$\tau^+ \tau^-$	3.7	3.3	$8.3 \cdot 10^{-15}$	$2.1 \cdot 10^{21}$	$1.0 \cdot 10^{-6}$	$1.3 \cdot 10^{-3}$	$5.5 \cdot 10^{-7}$
	$W^+ W^-$	3.6	3.3	$8.4 \cdot 10^{-15}$	$7.5 \cdot 10^{21}$	$4.3 \cdot 10^{-6}$	$5.4 \cdot 10^{-3}$	$7.5 \cdot 10^{-7}$
1000.0	$b\bar{b}$	4.5	3.1	$8.8 \cdot 10^{-15}$	$6.2 \cdot 10^{22}$	$3.4 \cdot 10^{-5}$	$4.2 \cdot 10^{-2}$	$5.6 \cdot 10^{-6}$
	$\tau^+ \tau^-$	3.6	3.4	$8.4 \cdot 10^{-15}$	$2.1 \cdot 10^{21}$	$1.2 \cdot 10^{-6}$	$1.5 \cdot 10^{-3}$	$5.4 \cdot 10^{-7}$
	$W^+ W^-$	3.4	3.4	$8.4 \cdot 10^{-15}$	$7.4 \cdot 10^{21}$	$4.3 \cdot 10^{-6}$	$5.4 \cdot 10^{-3}$	$5.8 \cdot 10^{-7}$

Table 1: Half-cone angles γ , upper 90% limits on the number of signal events N_S^{90} , the muon flux Φ_μ , the dark matter annihilation rate in the Sun Γ_A , the dark matter -proton spin-dependent $\sigma_{\chi p}^{SD}$ and spin-independent $\sigma_{\chi p}^{SI}$ scattering cross sections and neutrino fluxes Φ_ν .

interval $10 \div 1000$ GeV. The best value for the upper limit on SD elastic cross section is about 3×10^{-4} picobarn for masses of dark matter particle within $100 \div 200$ GeV, that is comparable with those presented by other operating neutrino telescopes. At the same time in the range of low masses of dark matter particle $10 \div 50$ GeV the Baksan limits on SD elastic cross section in the case of $\tau^+ \tau^-$ annihilation channel are the most stringent to date among the results obtained by neutrino telescopes.

Acknowledgments

We acknowledge our colleagues from the Baksan Observatory V.Petkov, Yu.Novoseltsev, R.Novoseltseva, V.Volchenko and A.Yanin for partnership in providing a long-term stability of the operating telescope. S.D. thanks D.Gorbunov for valuable discussions. We are grateful to a referee for very valuable advices and comments. We also acknowledge support from Federal Program "Researches and developments of priority directions of science and technology in Russia" under contract No. 16.518.11.7072. The work of S.D. was supported in part by the grants of the President of the Russian Federation NS-5590.2012.2, MK-2757.2012.2, by Russian Foundation for Basic Research grants 11-02-01528-a, 12-02-31726-mol-a and 13-02-01127 and by the Ministry of Science and Education under contract No. 8412. The numerical part of the work was performed on Computational Cluster of the Theory Division of INR RAS.

References

- [1] F. Zwicky, "Die Rotverschiebung von extragalaktischen Nebeln," *Helv. Acta* 6 (1933) 110.
- [2] G. Jungman, M. Kamionkowski and K. Griest, "Supersymmetric dark matter", *Phys. Rept.* **267** (1996), 195, [arXiv:hep-ph/9506380].
- [3] L. Bergstrom, "Non-baryonic dark matter: Observational evidence and detection methods", *Rept. Prog. Phys.* 63 (2000) 793, arXiv:hep-ph/0002126.
- [4] C. Munoz, "Dark matter detection in the light of recent experimental results", *Int. J. Mod. Phys. A* 19 (2004) 3093, arXiv:hep-ph/0309346.
- [5] G. Bertone, D. Hooper, J. Silk, "Particle dark matter: Evidence, candidates and constraints", *Phys. Rept.* **405** (2005) 279 [arXiv:hep-ph/0404175].
- [6] D. Clowe, M. Bradac, A. H. Gonzalez, M. Markevitch, S. W. Randall, C. Jones, D. Zaritsky, "A direct empirical proof of the existence of dark matter", *Astrophys.J.* 648, (2006), L109; D. Clowe, S. W. Randall and M. Markevitch, "Catching a bullet: direct evidence for the existence of dark matter", *Nucl.Phys.Proc.Suppl.* 173, (2007), 28;
- [7] J.P. Dietrich *et al.*, "A filament of dark matter between two clusters of galaxies", [arXiv:astro-ph/1207.0809]; D. Clowe *et al.*, "On dark peaks and missing mass: a weak lensing mass reconstruction of the merging cluster system 520", [arXiv:astro-ph/1209.2143] acc. by ApJ
- [8] N. Jarosik *et al.* [WMAP Collab.], "Seven-Year Wilkinson Microwave Anisotropy Probe (WMAP) Observations: Sky Maps, Systematic Errors, and Basic Results", *Astrophys.J.Suppl.* **192**, (2011) 14 [arXiv:astro-ph/1001.4744].
- [9] CMB Experiments, <http://lambda.gsfc.nasa.gov/product/expt/>
- [10] R. Bernabei *et al.*, [DAMA Collab.], "First results from DAMA/LIBRA and the combined results with DAMA/NaI", *Eur. Phys. J. C* **56** (2008) 333 [arXiv:astro-ph/0804.2741].
- [11] C. Savage, G. Gelmini, P. Gondolo and K. Freese, "Compatibility of DAMA/LIBRA dark matter detection with other searches," *JCAP* **0904** (2009) 010 [arXiv:0808.3607 [astro-ph]].

- [12] Z. Ahmed *et al.*, [CDMS Collab.], “Search for Weakly Interacting Massive Particles with the First Five-Tower Data from the Cryogenic Dark Matter Search at the Soudan Underground Laboratory”, *Phys. Rev. Lett.***102** (2009) 011301; Z. Ahmed *et al.* [CDMS Collab.], “Results from the Final Exposure of the CDMS II Experiment,” [arXiv:astro-ph/0912.3592].
- [13] C.E. Aalseth *et al.*, “Results from a Search for Light-Mass Dark Matter with a P-type Point Contact Germanium Detector”, *Phys. Rev. Lett.* **106** (2011) 131301 [arXiv:1002.4703 [astro-ph.CO]].
- [14] G. Angloher, M. Bauer, I. Bavykina, A. Bento, C. Bucci, C. Ciemiak, G. Deuter and F. von Feilitzsch *et al.*, “Results from 730 kg days of the CRESST-II Dark Matter Search,” *Eur. Phys. J. C* **72** (2012) 1971 [arXiv:1109.0702 [astro-ph.CO]].
- [15] S. Profumo, P. Ullio, “Multi-wavelength Searches for Particle Dark Matter”, Chapter 27 of “Particle Dark Matter: Observations, Models and Searches” ed. Gianfranco Bertone, 2010, Cambridge University Press, arXiv:1001.4086v1 [astro-ph.HE]
- [16] T. Tanaka *et al.* [Super-Kamiokande Collaboration], “An Indirect Search for WIMPs in the Sun using 3109.6 days of upward-going muons in Super-Kamiokande”, *Astrophys. J.* **742**, 78, (2011)[arXiv:1108.3384 [astro-ph.HE]].
- [17] M. G. Aartsen *et al.* [IceCube Collaboration], “Search for dark matter annihilations in the Sun with the 79-string IceCube detector,” *Phys. Rev. Lett.* **110**, 131302, (2013) [arXiv:1212.4097 [astro-ph.HE]].
- [18] S. Adrian-Martinez *et al.* [ANTARES Collaboration], “First Search for Dark Matter Annihilation in the Sun Using the ANTARES Neutrino Telescope,” arXiv:1302.6516v1 [astro-ph.HE].
- [19] E.N. Alekseev, V.V. Alexeyenko, Yu.M. Andreyev, V.N. Bakatanov *et al.*, “Baksan Underground Scintillation Telescope”, 16th ICRC, **v.10**, 276, (1979), Edited by Saburo Miyake, <http://adsabs.harvard.edu/abs/1979ICRC...10..276A>
- [20] M.M. Boliev, E.V. Bugaev, A.V. Butkevich, A.E. Chudakov, S.P. Mikheyev, O.V. Suvorova and V.N. Zakidyshev, “BAKSAN NEUTRALINO SEARCH”, *Dark Matter in Astro- and Particle Physics*, edited by H.V.Klapdor-Kleingrothaus and Y.Ramachers (Singapore: World Sci.), (1997), 711.
- [21] M.M. Boliev, E.V. Bugaev, A.V. Butkevich, A.E. Chudakov, S.P. Mikheyev, O.V. Suvorova and V.N. Zakidyshev, “Search for supersymmetric dark matter with Baksan Underground Telescope”, *Nucl. Phys.*, **48**, 83, (1996).
- [22] M.M. Boliev, A.N. Butkevich, A.E. Chudakov, S.P. Mikheyev, O.V. Suvorova, V.N. Zakidyshev, “Observation of upward through-going muons with the Baksan detector: an update”, *Nucl. Phys.*, **70**, 371, (1999).
- [23] J. Beringer *et al.*, (Particle Data Group), *Phys. Rev. D***86**, 010001 (2012)
- [24] J. Edsjo, WimpSim Neutrino Monte Carlo, <http://www.fysik.su.se/~edsjo/wimpsim/>
- [25] M. Blennow, J. Edsjo and T. Ohlsson, “Neutrinos from WIMP annihilations using a full three-flavor Monte Carlo,” *JCAP* **0801** (2008) 021 [arXiv:0709.3898 [hep-ph]].

- [26] A.E. Chudakov, B.A. Makoev, Yu.V. Malovichko, V.Ya. Markov, S.P. Mikheyev, V.I. Stepanov, V.N. Zakidyshev, “Study of High Energy Cosmic Ray Neutrinos. Status and Possibilities of Baksan Underground Scintillation Telescope”, 16th ICRC, **v.10**, 287, (1979), Edited by Saburo Miyake, <http://adsabs.harvard.edu/abs/1979ICRC...10..287C>
- [27] Yu.M. Andreyev, A.E. Chudakov, B.A. Makoev, Yu.V. Malovichko, V.Ya. Markov, S.P. Mikheyev, V.I. Stepanov, V.N. Zakidyshev, “Speed Distribution of Penetrating Particles at the Depth 850 hg/cm²”, 16th ICRC, **v.10**, 184, (1979), Edited by Saburo Miyake, <http://adsabs.harvard.edu/abs/1979ICRC...10..184A>
- [28] Yu.M. Andreyev, Determination of characteristics of the muon trajectories at the Baksan Underground Scintillator Telescope and a search for a signal from the Cygnus-X3, PhD thesis in Russian, Moscow, (1989).
- [29] Yu.M. Andreyev, V.I. Gurentsov, I.M. Kogai, O.Yu. Nikishina, The angular resolution of the Baksan Underground Scintillator Telescope, INR preprint in Russian, Num. 1253, Moscow, (1989).
- [30] S.N. Karpov, Muon cosmic rays intensity variations, arising due to the Moon and the Sun, PhD thesis in Russian, Moscow, (2001).
- [31] Yu.M. Andreyev, V.N. Zakidyshev, S.N. Karpov, V.N. Khodov, Observation of the Moon Shadow in Cosmic Ray Muons, Cosmic Research, **v.40**, Issue 6, 559, (2002), <http://link.springer.com/article/10.1023%2FA%3A1021553713199>.
- [32] V.N. Zakidyshev, A seach for local sources of high energy neutrinos with data of the Baksan Underground Scintillator Telescope, PhD thesis in Russian, Moscow, (1996).
- [33] M.M. Boliev, A.N. Butkevich, A.E. Chudakov, B.A. Makoev, S.P. Mikheyev, V.N. Zakidyshev, “ ν_μ -Flux as Measured by Baksan Underground Telescope”, Proc. of the 17th ICRC, Paris, France, **v.7**, 106, (1981), <http://adsabs.harvard.edu/abs/1981ICRC....7..106B>
- [34] M.M. Boliev, A.V. Butkevich, S.P. Mikheyev and O.V. Suvorova, “Results with the Baksan neutrino telescope”, Proc. of the First Workshop on Exotic Physics with Neutrino Telescope, Uppsala, Sweden, 19 (2006) [arXiv:astro-ph/0701333].
- [35] P.T.Walance, Starlink user note 67 (1999), <http://star-www.rl.ac.uk/star/docs/sun67.htx/sun67.html>.
- [36] Particle Data Group, Phys. Rev. D **45** (1992)
- [37] M. Cirelli, N. Fornengo, T. Montaruli, I. A. Sokalski, A. Strumia and F. Vissani, “Spectra of neutrinos from dark matter annihilations,” Nucl. Phys. B **727** (2005) 99 [Erratum-ibid. B **790** (2008) 338] [hep-ph/0506298].
- [38] T. Ohlsson and H. Snellman, “Three flavor neutrino oscillations in matter,” J. Math. Phys. **41** (2000) 2768 [Erratum-ibid. **42** (2001) 2345] [hep-ph/9910546].
- [39] T. Ohlsson and H. Snellman, “Neutrino oscillations with three flavors in matter of varying density,” Eur. Phys. J. C **20** (2001) 507 [hep-ph/0103252].
- [40] J. N. Bahcall, A. M. Serenelli and S. Basu, “New solar opacities, abundances, helioseismology, and neutrino fluxes,” Astrophys. J. **621** (2005) L85 [astro-ph/0412440].

- [41] D. V. Forero, M. Tortola and J. W. F. Valle, “Global status of neutrino oscillation parameters after Neutrino-2012,” *Phys. Rev. D* **86** (2012) 073012 [arXiv:1205.4018 [hep-ph]].
- [42] K. Griest and D. Seckel, “Cosmic Asymmetry, Neutrinos and the Sun,” *Nucl. Phys. B* **283** (1987) 681 [Erratum-ibid. *B* **296** (1988) 1034].
- [43] E. A. Paschos and J. Y. Yu, “Neutrino interactions in oscillation experiments,” *Phys. Rev. D* **65** (2002) 033002 [hep-ph/0107261].
- [44] J. Pumplin, D. R. Stump, J. Huston, H. L. Lai, P. M. Nadolsky and W. K. Tung, “New generation of parton distributions with uncertainties from global QCD analysis,” *JHEP* **0207** (2002) 012 [hep-ph/0201195].
- [45] V. Barger, W. -Y. Keung, G. Shaughnessy and A. Tregre, “High energy neutrinos from neutralino annihilations in the Sun,” *Phys. Rev. D* **76** (2007) 095008 [arXiv:0708.1325 [hep-ph]].
- [46] P. Lipari and T. Stanev, *Phys. Rev. D* **44** (1991) 3543.
- [47] E. V. Bugaev, A. Misaki, V. A. Naumov, T. S. Sinegovskaya, S. I. Sinegovsky and N. Takahashi, *Phys. Rev. D* **58** (1998) 054001 [hep-ph/9803488].
- [48] Donald E. Groom, Nikolai V. Mokhov, Sergei I. Striganov, Muon stopping power and range tables 10 MeV-100 TeV, *Atomic Data and Nuclear Data Tables*, **78** (2001) 183-356
- [49] A. E. Erkoca, M. H. Reno and I. Sarcevic, “Muon Fluxes From Dark Matter Annihilation,” *Phys. Rev. D* **80** (2009) 043514 [arXiv:0906.4364 [hep-ph]].
- [50] A. V. Butkevich, “Energy spectrum of cosmic rays neutrinos and bounds on neutrino oscillation parameters,” PhD thesis in Russian, (1991), Moscow.
- [51] G. C. Hill and K. Rawlins, “Unbiased cut selection for optimal upper limits in neutrino detectors: The Model rejection potential technique,” *Astropart. Phys.* **19** (2003) 393 [astro-ph/0209350].
- [52] G. Wikstrom and J. Edsjo, “Limits on the WIMP-nucleon scattering cross-section from neutrino telescopes,” *JCAP* **0904** (2009) 009 [arXiv:0903.2986 [astro-ph.CO]].
- [53] S. Demidov and O. Suvorova, “Annihilation of NMSSM neutralinos in the Sun and neutrino telescope limits,” *JCAP* **1006** (2010) 018 [arXiv:1006.0872 [hep-ph]].
- [54] A. Gould, “Cosmological density of WIMPs from solar and terrestrial annihilations,” *Astrophys. J.* **388** (1992) 338. A. Gould, “Resonant Enhancements In Wimp Capture By The Earth,” *Astrophys. J.* **321** (1987) 571.
- [55] M. G. Kostyuk, V. B. Petkov, R. V. Novoseltseva et al., “Variations of the high energy muon flux and space-time structure of the temperature profile in the atmosphere”, *J.Phys: Conf. Ser.* **409** 012231 (2013), doi:10.1088/1742-6596/409/1/012231
- [56] A. Cooper-Sarkar, P. Mertsch and S. Sarkar, “The high energy neutrino cross-section in the Standard Model and its uncertainty,” *JHEP* **1108** (2011) 042 [arXiv:1106.3723 [hep-ph]].
- [57] C. Rott, T. Tanaka and Y. Itow, “Enhanced Sensitivity to Dark Matter Self-annihilations in the Sun using Neutrino Spectral Information,” *JCAP* **1109** (2011) 029 [arXiv:1107.3182 [astro-ph.HE]].

- [58] R. Catena and P. Ullio, “A novel determination of the local dark matter density,” *JCAP* **1008** (2010) 004 [arXiv:0907.0018 [astro-ph.CO]].
- [59] R. D. Cousins and V. L. Highland, “Incorporating systematic uncertainties into an upper limit,” *Nucl. Instrum. Meth. A* **320** (1992) 331.
- [60] <http://dmtools.brown.edu>
- [61] G. Lambard for [ANTARES Collaboration], “Indirect dark matter search with the ANTARES neutrino telescope”, PoS(DSU2012).
- [62] P. Coyle, “Recent results from the ANTARES deep sea neutrino telescope,” *Nucl. Phys. Proc. Suppl.* **235-236** (2013) 339 [arXiv:1212.2416 [astro-ph.HE]].
- [63] S. Archambault *et al.* [PICASSO Collaboration], “Constraints on Low-Mass WIMP Interactions on ^{19}F from PICASSO,” *Phys. Lett. B* **711** (2012) 153 [arXiv:1202.1240 [hep-ex]].
- [64] S. C. Kim, H. Bhang, J. H. Choi, W. G. Kang, B. H. Kim, H. J. Kim, K. W. Kim and S. K. Kim *et al.*, “New Limits on Interactions between Weakly Interacting Massive Particles and Nucleons Obtained with CsI(Tl) Crystal Detectors,” *Phys. Rev. Lett.* **108** (2012) 181301 [arXiv:1204.2646 [astro-ph.CO]].
- [65] M. Felizardo, T. A. Girard, T. Morlat, A. C. Fernandes, A. R. Ramos, J. G. Marques, A. Kling and J. Puibasset *et al.*, “Final Analysis and Results of the Phase II SIMPLE Dark Matter Search,” *Phys. Rev. Lett.* **108** (2012) 201302 [arXiv:1106.3014 [astro-ph.CO]].
- [66] S. Chatrchyan *et al.* [CMS Collaboration], “Search for dark matter and large extra dimensions in monojet events in pp collisions at $\sqrt{s} = 7$ TeV,” *JHEP* **1209** (2012) 094 [arXiv:1206.5663 [hep-ex]].
- [67] G. Aad *et al.* [ATLAS Collaboration], “Search for dark matter candidates and large extra dimensions in events with a jet and missing transverse momentum with the ATLAS detector,” *JHEP* **1304** (2013) 075 [arXiv:1210.4491 [hep-ex]].
- [68] E. Aprile *et al.* [XENON100 Collaboration], “Limits on spin-dependent WIMP-nucleon cross sections from 225 live days of XENON100 data,” arXiv:1301.6620 [astro-ph.CO].
- [69] G. Aad *et al.* [ATLAS Collaboration], “Search for dark matter candidates and large extra dimensions in events with a photon and missing transverse momentum in pp collision data at $\sqrt{s} = 7$ TeV with the ATLAS detector,” *Phys. Rev. Lett.* **110** (2013) 011802 [arXiv:1209.4625 [hep-ex]].
- [70] S. Chatrchyan *et al.* [CMS Collaboration], “Search for Dark Matter and Large Extra Dimensions in pp Collisions Yielding a Photon and Missing Transverse Energy,” *Phys. Rev. Lett.* **108** (2012) 261803 [arXiv:1204.0821 [hep-ex]].
- [71] J. Goodman, M. Ibe, A. Rajaraman, W. Shepherd, T. M. P. Tait and H. -B. Yu, “Constraints on Dark Matter from Colliders,” *Phys. Rev. D* **82** (2010) 116010 [arXiv:1008.1783 [hep-ph]].
- [72] P. J. Fox, R. Harnik, J. Kopp and Y. Tsai, “Missing Energy Signatures of Dark Matter at the LHC,” *Phys. Rev. D* **85** (2012) 056011 [arXiv:1109.4398 [hep-ph]].
- [73] A. Rajaraman, W. Shepherd, T. M. P. Tait and A. M. Wijangco, “LHC Bounds on Interactions of Dark Matter,” *Phys. Rev. D* **84** (2011) 095013 [arXiv:1108.1196 [hep-ph]].

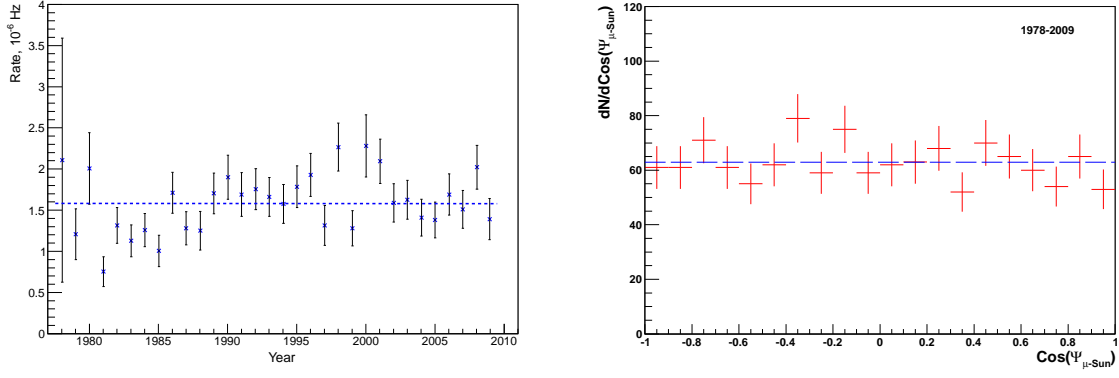


Figure 1: Left: Measured rate of upward through going muons at the BUST since December 1978. Right: Distribution of measured events in angle $\Psi_{\mu-\text{Sun}}$ between incoming muon events at the BUST and the Sun position. The direction of the Sun corresponds to $\cos \Psi_{\mu-\text{Sun}} = 1$.

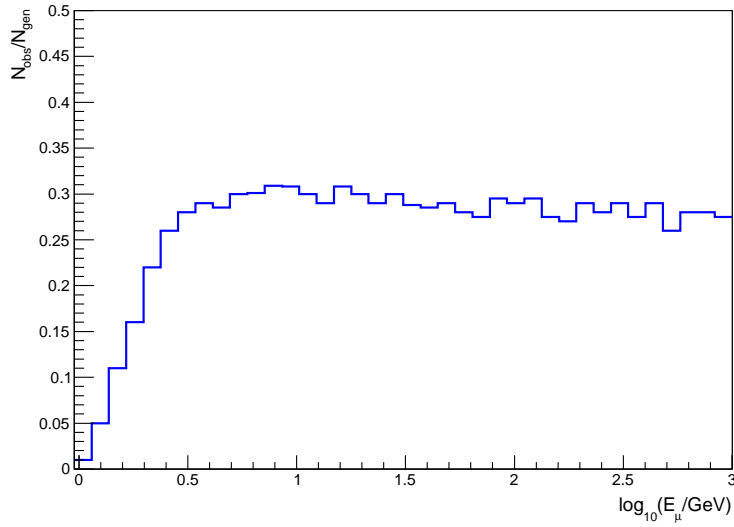


Figure 2: The ratio of the number of MC events which survive all cuts (N_{obs}) and total MC generated neutrino interactions (N_{gen}) in the Baksan surrounding rock in dependence on muon energy.

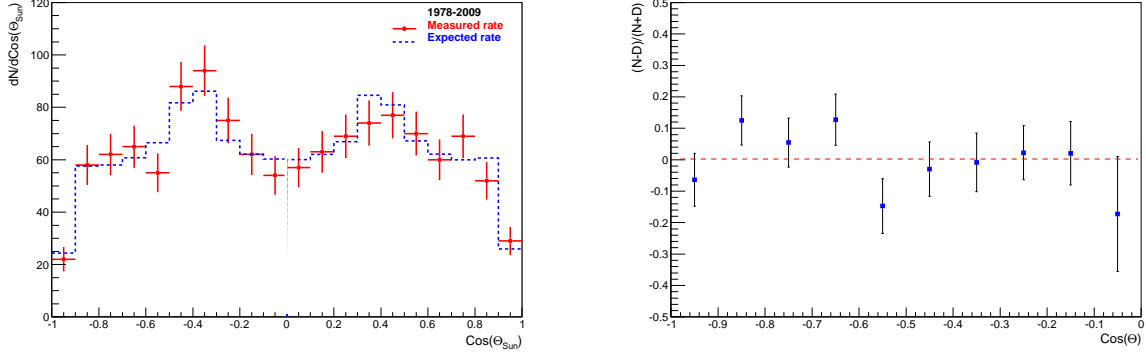


Figure 3: Left: The integral rate of 1255 selected upward through going muons as a function of zenith angle of the Sun for the BUST measured time of good data periods (red points with error bars) and expected one for the detector runtime (blue histogram). The later is normalized to this number of events. Right: Zenith distribution for asymmetry $\frac{N-D}{N+D}$ between the number of neutrino events coming at time when the Sun is under (night, N) or above (day, D) the horizon.

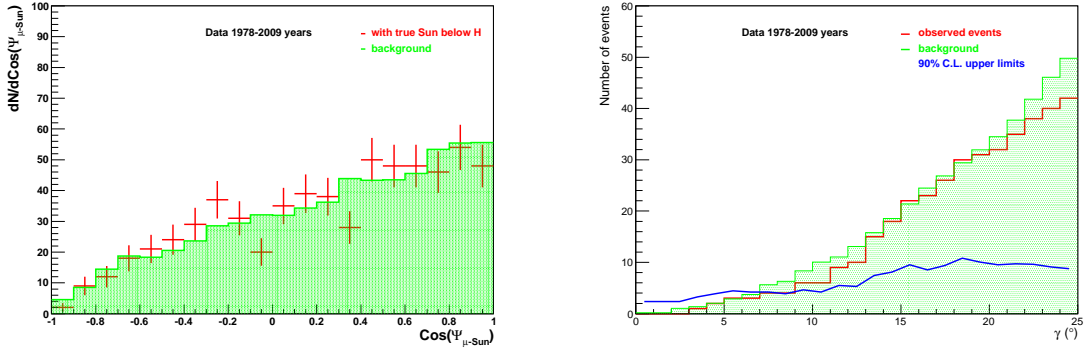


Figure 4: Left: Distributions of $\cos \Psi_{\mu-\text{Sun}}$ for events toward true Sun position below horizon (red) in comparison with measured background (green) obtained from the distributions for $\cos \Psi_{\mu-\text{Sun}}$ averaged over six shifted Sun positions. Right: The 90% C.L. upper limits on additional number of upward going muon events in the direction toward the Sun (blue) in cone half-angle γ . Measured (red) and background (green) events are also shown depending on the value of γ .

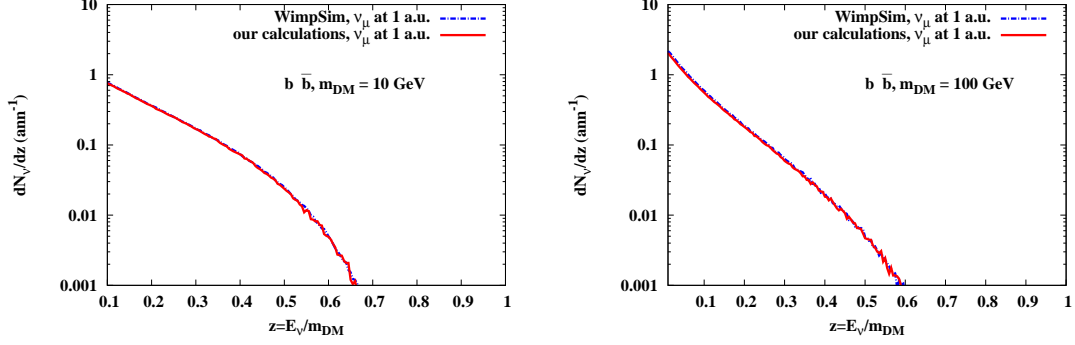


Figure 5: The energy spectra of ν_μ neutrino at production point and at the distance $R=1$ a.u. from the Sun obtained with the help of WimpSim package and by our calculations for $b\bar{b}$ annihilation channels and $m_{\text{DM}} = 10$ GeV (left) and 100 GeV (right).

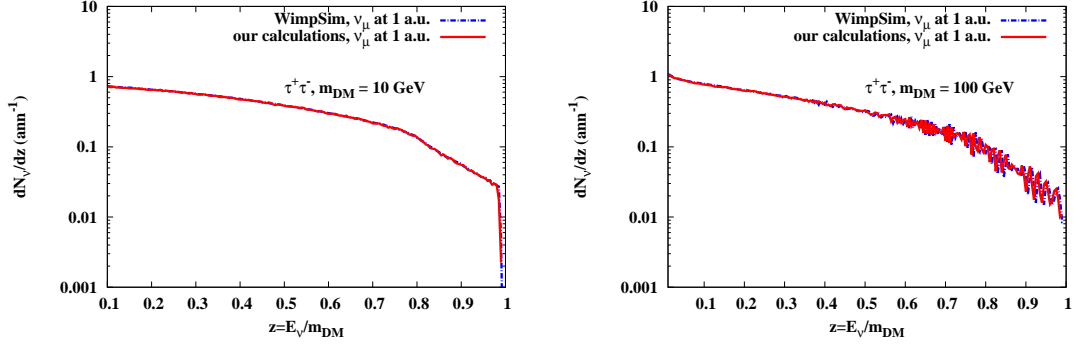


Figure 6: The energy spectra of ν_τ neutrino at production point and ν_μ neutrino at the distance $R = 1$ a.u. from the Sun obtained with the help of WimpSim package and by our calculations for $\tau^+\tau^-$ annihilation channels and $m_{\text{DM}} = 10$ GeV (left) and 100 GeV (right).

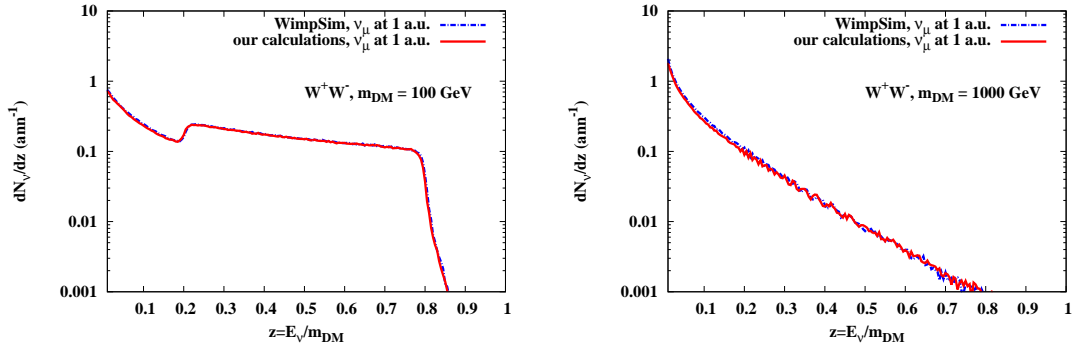


Figure 7: The energy spectra of ν_τ neutrino at production point and ν_μ neutrino at the distance $R = 1$ a.u. from the Sun obtained with the help of WimpSim package and by our calculations for W^+W^- annihilation channels and $m_{\text{DM}} = 100$ GeV (left) and 1000 GeV (right).

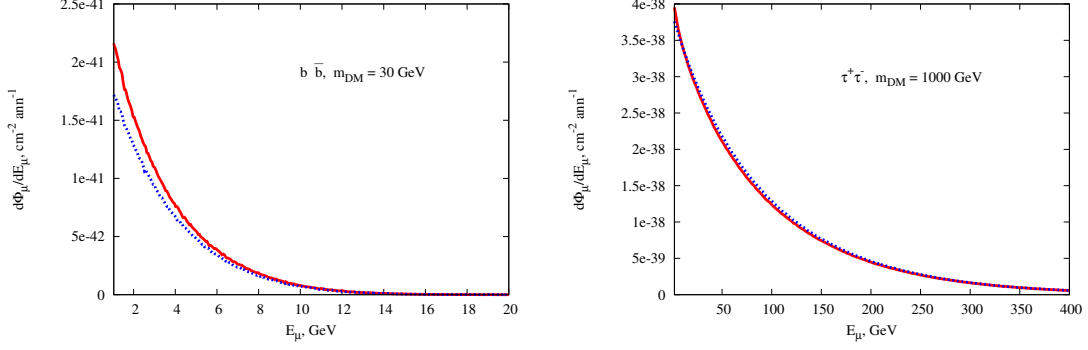


Figure 8: The comparison between muon energy spectra obtained taking into account energy dependence for $\alpha(E)$ and $\beta(E)$ (red, solid line) and using constant values $\alpha(E) \approx 2.2 \cdot 10^{-3} \text{ GeV} \cdot \text{cm}^2/\text{g}$ and $\beta(E) \approx 4.4 \cdot 10^{-6} \text{ cm}^2/\text{g}$ (blue, dotted line).

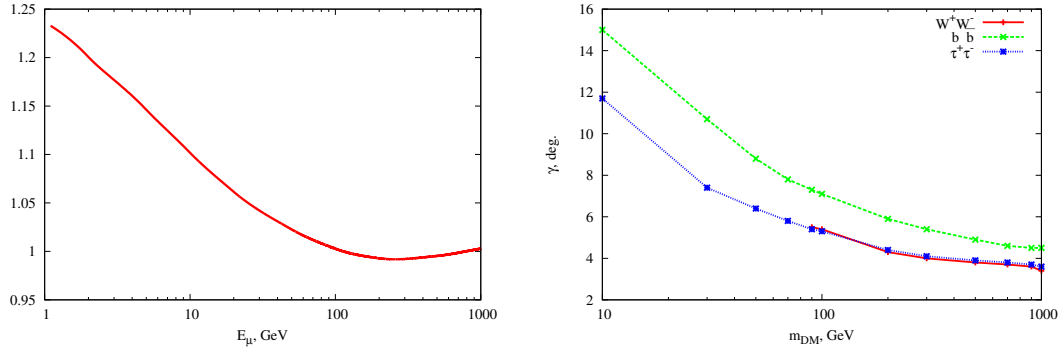


Figure 9: Left: The ratio of muon ranges calculated using full energy dependence for $\alpha(E)$ and $\beta(E)$ and using constant values $\alpha(E) \approx 2.2 \cdot 10^{-3} \text{ GeV} \cdot \text{cm}^2/\text{g}$ and $\beta(E) \approx 4.4 \cdot 10^{-6} \text{ cm}^2/\text{g}$. Right: Cone half-angle γ as a function of the mass m_{DM} for three annihilations channels $b\bar{b}$, $\tau^+\tau^-$ and W^+W^- .

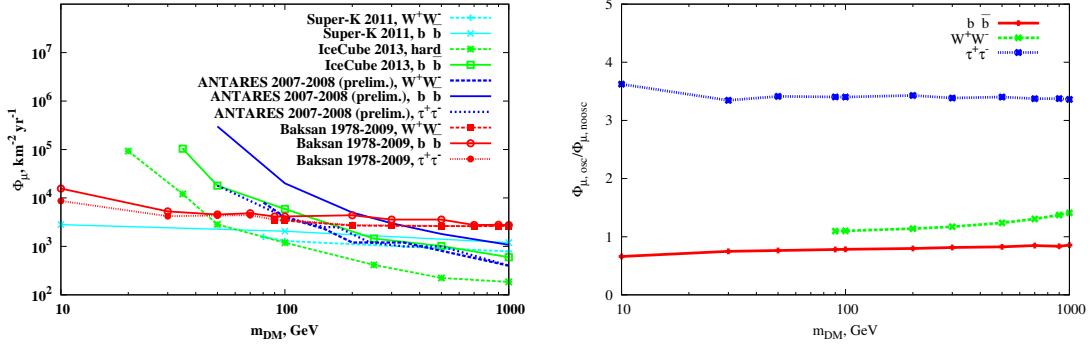


Figure 10: The Baksan limits on muon flux from the dark matter annihilations in the Sun in comparison with other experimental results (left); ratios of expected muon fluxes both from DM neutrino and antineutrino generated in pure three annihilation branches $b\bar{b}$ quarks, or $\tau^+\tau^-$ leptons or W^+W^- bosons in cases with and without three flavours oscillations (right).

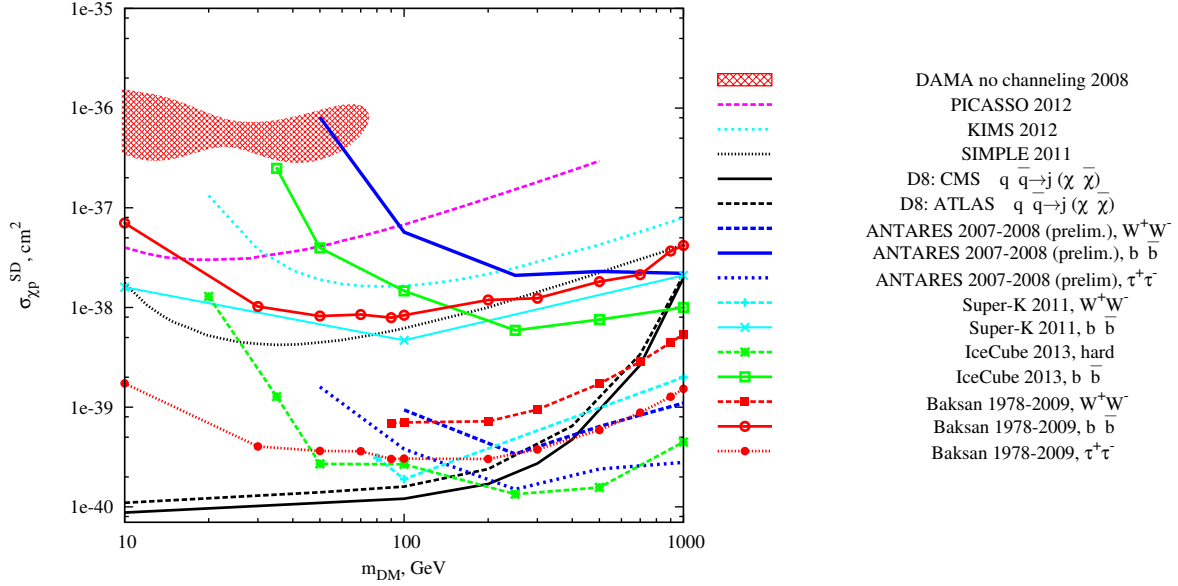


Figure 11: The Baksan limits on SD elastic cross section of dark matter particle on proton in comparison with other experimental results. We implement the DMTools [60] database to plot the results of direct searches.

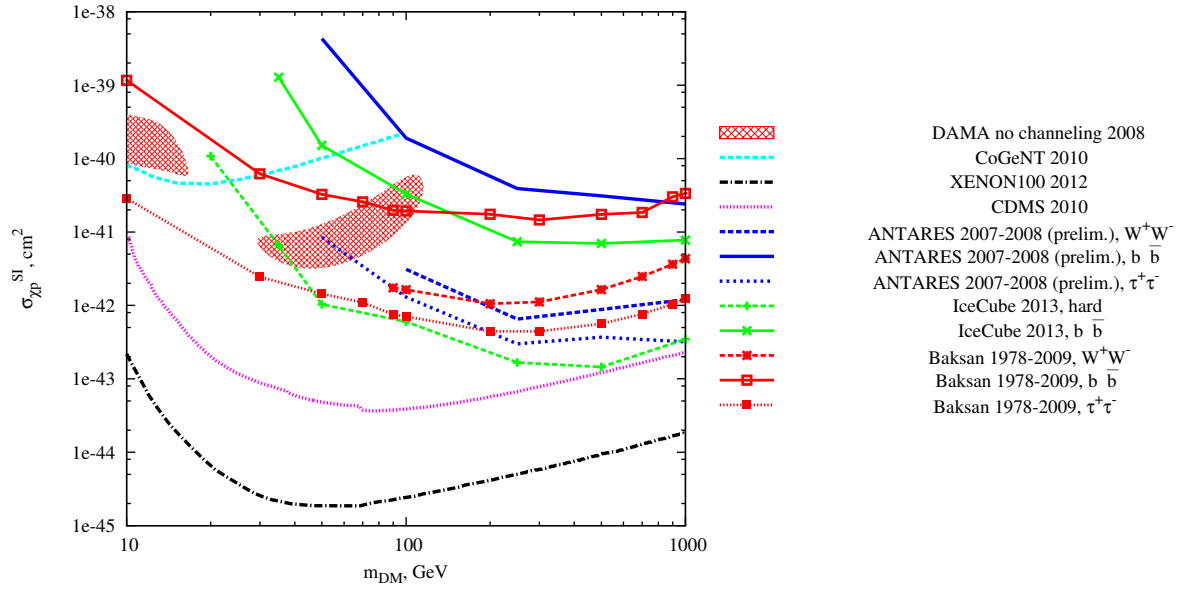


Figure 12: The Baksan limits on SI elastic cross section of dark matter particle on proton in comparison with other experimental results. We implement the DMTools [60] database to plot the results of direct searches.